BRAIN
A JOURNAL OF NEUROLOGY

Movement-related dynamics of cortical oscillations in Parkinson's disease and essential tremor

Efstathios D. Kondylis,[1] Michael J. Randazzo,[1] Ahmad Alhourani,[1] Witold J. Lipski,[1] Thomas A. Wozny,[1] Yash Pandya,[1] Avniel S. Ghuman,[1,2,3,4] Robert S. Turner,[2,3,4] Donald J. Crammond[1] and R. Mark Richardson[1,2,3,4]

Recent electrocorticography data have demonstrated excessive coupling of beta-phase to gamma-amplitude in primary motor cortex and that deep brain stimulation facilitates motor improvement by decreasing baseline phase-amplitude coupling. However, both the dynamic modulation of phase-amplitude coupling during movement and the general cortical neurophysiology of other movement disorders, such as essential tremor, are relatively unexplored. To clarify the relationship of these interactions in cortical oscillatory activity to movement and disease state, we recorded local field potentials from hand sensorimotor cortex using subdural electrocorticography during a visually cued, incentivized handgrip task in subjects with Parkinson's disease ($n = 11$), with essential tremor ($n = 9$) and without a movement disorder ($n = 6$). We demonstrate that abnormal coupling of the phase of low frequency oscillations to the amplitude of gamma oscillations is not specific to Parkinson's disease, but also occurs in essential tremor, most prominently for the coupling of alpha to gamma oscillations. Movement kinematics were not significantly different between these groups, allowing us to show for the first time that robust alpha and beta desynchronization is a shared feature of sensorimotor cortical activity in Parkinson's disease and essential tremor, with the greatest high-beta desynchronization occurring in Parkinson's disease and the greatest alpha desynchronization occurring in essential tremor. We also show that the spatial extent of cortical phase-amplitude decoupling during movement is much greater in subjects with Parkinson's disease and essential tremor than in subjects without a movement disorder. These findings suggest that subjects with Parkinson's disease and essential tremor can produce movements that are kinematically similar to those of subjects without a movement disorder by reducing excess sensorimotor cortical phase-amplitude coupling that is characteristic of these diseases.

1 Department of Neurological Surgery, University of Pittsburgh School of Medicine, Pittsburgh, PA, USA
2 Department of Neurobiology, University of Pittsburgh School of Medicine, Pittsburgh, PA, USA
3 Center for the Neural Basis of Cognition, University of Pittsburgh, Pittsburgh, PA, USA
4 University of Pittsburgh Brain Institute, Pittsburgh, PA, USA

Correspondence to: Mark Richardson, MD, PhD,
Department of Neurological Surgery,
University of Pittsburgh Medical Center 200 Lothrop St.,
Suite B400, Pittsburgh, PA 15217 USA
E-mail: richardsonrm@upmc.edu

Introduction

The adaptation of electrocorticography (ECoG) for intraoperative neurophysiology research in subjects undergoing deep brain stimulation (DBS) for movement disorders is a recent and important contribution to human systems neuroscience research. This method employs a subdural strip electrode, introduced through the skull opening required for DBS lead implantation, to record cortical local field potentials during the awake portion of the procedure. Starr and colleagues used this technique to demonstrate disease-specific differences in sensorimotor cortex local field potentials in subjects with Parkinson's disease, primary craniocervical dystonia and essential tremor (Crowell *et al.*, 2012). Cortical beta activity was not significantly greater in subjects with Parkinson's disease, confirming that the excessive beta (13–30 Hz) activity characteristically observed in the subthalamic nucleus in Parkinson's disease is not represented at the cortical level (Bosboom *et al.*, 2006). Broadband gamma (50–200 Hz) spectral power, however, was found to be increased in Parkinson's disease. The relevance of this finding was indicated in follow-up studies demonstrating that beta-phase is excessively coupled to gamma-amplitude in primary motor cortex in Parkinson's disease subjects compared to those with craniocervical dystonia or no movement disorder (de Hemptinne *et al.*, 2013), an interaction that is reversibly reduced by therapeutic DBS of the subthalamic nucleus (de Hemptinne *et al.*, 2015).

Essential tremor is also a movement disorder in which symptomatology may correlate to abnormal cortical oscillatory activity. Coherence at tremor frequency between sensorimotor cortex and surface EMG has been reported using EEG (Hellwig *et al.*, 2001), MEG (Raethjen *et al.*, 2007; Schnitzler *et al.*, 2009), and ECoG (Air *et al.*, 2012), although this coherence is not observed in every subject. Whether phase-amplitude coupling is abnormal in essential tremor has not been reported. Likewise, movement-related modulation of cortical neural dynamics has not been compared between subjects with Parkinson's disease, essential tremor, and no movement disorder. Previous work has shown that the initiation of movement is accompanied by desynchronization of cortical alpha and beta activity (movement related desynchronization), synchronization of cortical high frequency activity (50–200 Hz) (Jasper and Penfield, 1949; Crone *et al.*, 1998*a*, *b*), and reduction of cortical phase-amplitude coupling (Miller *et al.*, 2012; Yanagisawa *et al.*, 2012). To determine the extent to which movement-related cortical oscillatory dynamics are altered in subjects with essential tremor or Parkinson's disease, we recorded local field potential from pre- and postcentral sensorimotor cortex during an instructed delay, visually cued, monetary incentive handgrip task in subjects undergoing DBS lead implantation. A novel method (Randazzo *et al.*, 2016), which was validated in a previous study using a portion of the high-frequency activation data reported here (Kondylis *et al.*, 2016), was applied to localize the subdural electrodes accurately and precisely on the cortical surface. We then compared these results to those from subjects without a movement disorder who were undergoing intracranial monitoring for seizure mapping.

Materials and methods

Subjects

Study subjects with movement disorders were recruited from a population of patients with Parkinson's disease or essential tremor scheduled to undergo deep brain stimulator implantation. The non-movement disorder group comprised patients with epilepsy undergoing intracranial monitoring for seizure localization for whom there was no evidence of ictal or inter-ictal epileptiform activity in sensorimotor cortex. All subjects were recommended for surgery by their respective multidisciplinary review board based on standard clinical indications and inclusion/exclusion criteria. See Table 1 for full demographic description of subjects. All participants provided written, informed consent in accordance with a protocol approved by the Institutional Review Board of the University of Pittsburgh (IRB Protocol # PRO13110420).

Behavioural paradigm

Subjects were positioned in a semi-seated position with an unobstructed view of a 24" computer monitor positioned for comfortable viewing with a grip force lever (MIE medical research) in each hand. They performed a visually cued, instructed delay handgrip task with monetary incentive. A single trial of the task began with illumination of the yellow light on a traffic light in the center of the screen and an instructional cue on one side of the screen designating with which hand the subject should subsequently respond by squeezing the handgrip (Fig. 1). The instructional cue and yellow light remained illuminated for 1000–2000 ms, depending on each subject's cognitive ability to keep up with the task, after which the yellow light was extinguished and either the green light (Go cue) or red light (No-Go cue) was illuminated. Following a Go cue, subjects successfully completed the trial if they responded with the correct hand in ⩽2 s and maintained at least 10% of their previously measured maximum voluntary grip force for ⩾100 ms. A trial was counted as an error if subjects did not meet these criteria, or inappropriately squeezed during a No-Go trial. Following completion of each trial, a feedback message cued the subject to stop squeezing the handgrip and indicated the winnings or losses for the trial as well as running balance of winnings. Each trial was followed by a variable intertrial interval of 500–1000 ms. Before consenting to perform the task, all subjects were informed that they would receive the monetary equivalent of their accrued winnings. The feedback of monetary earnings served as an indication of the subject's performance, and the monetary reward as an incentive to maximize performance. All subjects were given 10 min to practice and only performed the task intra-operatively if they achieved a proficiency of at least 75% correct trials during this practice period. Error and No-Go trials were not analyzed. Subjects performed the task for

Table I Clinical characteristics of study subjects

	ECoG Side	Age (years)	Gender	MMSE	Tremor score[a]	Rest tremor amplitude[b]	Postural tremor of the hands[b]	Finger tapping[b]	Hand movement[b]	RAM[b]
Control group										
Subject 1	L	31	F	NS						
Subject 2	L	19	M	30/30						
Subject 3	L	20	F	24/30						
Subject 4	L	46	M	29/30						
Subject 5	R	50	F	NR						
Subject 6	L	31	F	NR						
Essential tremor										
Subject 7	L	55	M	27/30	3					
Subject 8	L	66	M	29/30	3					
Subject 9	L	71	M	28/30	4					
Subject 10	R	73	M	NR	3					
Subject 11	L	68	M	27/30	3					
Subject 12	L	68	M	30/30	3					
Subject 13	L	78	F	30/30	3					
Subject 14	L	64	F	30/30	3					
Subject 15	R	71	M	28/30	3					
Parkinson's disease										
Subject 16	L	64	M	29/30		1	0	1	1	2
Subject 17	R	69	F	29/30		0	0	1	1	1
Subject 18	R	64	M	30/30		0	0	2	2	2
Subject 19	R	60	M	30/30		2	2	1	1	1
Subject 20	L	52	M	27/30[c]		NR	NR	NR	NR	NR
Subject 21	L	54	F	29/30		NR	NR	NR	NR	NR
Subject 22	L	78	F	NR		1	0	3	2	2
Subject 23	L	68	M	29/30		0	0	2	2	1
Subject 24	L	47	F	30/30		NR	NR	NR	NR	NR
Subject 25	L	66	M	30/30		3	2	3	3	3
Subject 26	L	71	M	30/30		2	0	3	3	3

MMSE = Mini-Mental State Examination for neurocognition; NR = value was not recorded in the medical record; RAM = rapid alternating movements of the hands.
[a]Fahn-Tolosa-Marin tremor score.
[b]Unified Parkinson's Disease Rating Scale motor subscores in the OFF medication state.
[c]Montreal Cognitive Assessment.
All movement disorder scale values are reported for the hand contralateral to the side of ECoG recording.

10 to 25 min and only subjects with >15 successful trials for each hand were analyzed.

Electrophysiological recordings

ECoG data were recorded intraoperatively from subjects with movement disorders using either a 1×6 ($n = 19$, 2.3 mm exposed electrode diameter, 10 mm inter-electrode distance) or a 2×14 ($n = 1$, 1.2 mm exposed electrode diameter, 4 mm inter-electrode distance) contact platinum iridium cortical strip electrodes (Ad-Tech, Medical Instrument Corporation) temporarily implanted through the burr hole used for DBS lead implantation (Crowell *et al.*, 2012). Burr hole locations were determined solely by standard selection of

a safe entry point for the intended DBS lead trajectory, with no additional exposure needed for ECoG electrode placement. During planning of the DBS trajectory, an additional point was planned that corresponded to the hand knob as visually identified on the preoperative MRI, and this location was marked on the scalp prior to creating the burr holes (Crowell *et al.*, 2012). ECoG electrodes were aimed in the direction of the scalp marking for the hand knob and steered there over a planned insertion distance equal to the measured distance from the burr hole to just posterior to the post-central sulcus. We have not collected pre-insertion ECoG in our practice, as once the dura is opened, we place the ECoG electrode and insert the guide tube to target as efficiently as possible, then seal the burr hole with gelfoam and fibrin glue to
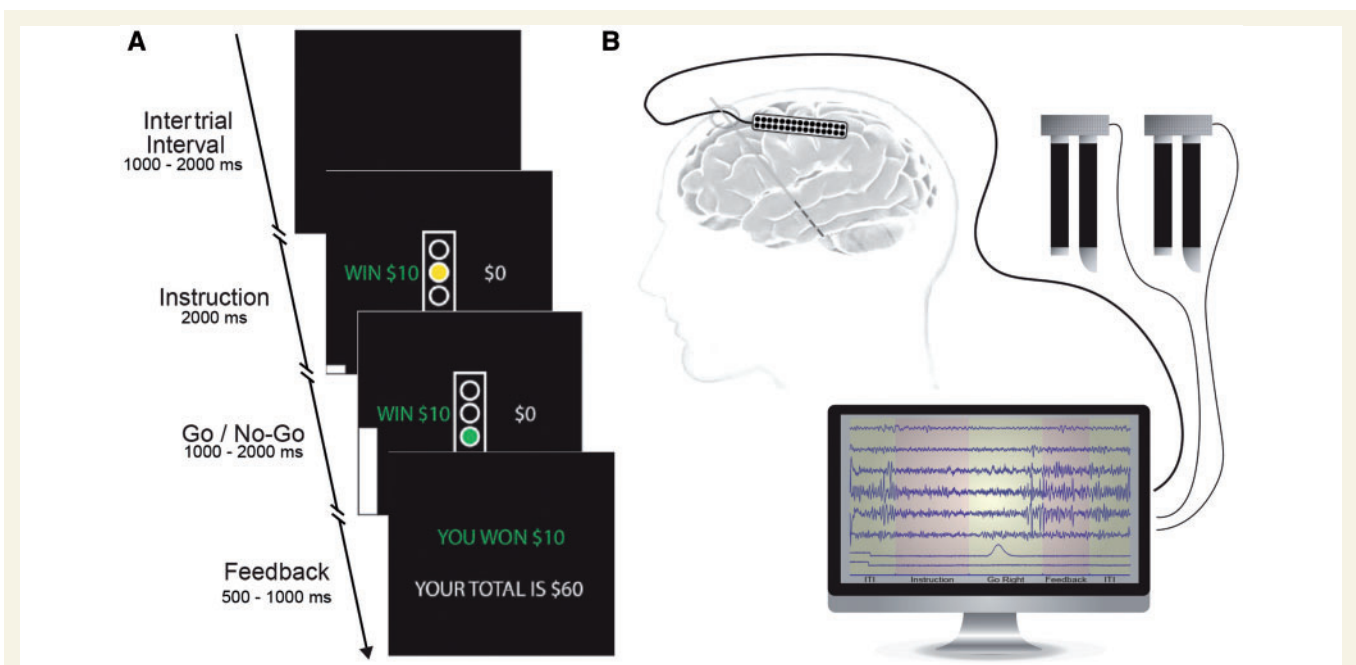
Figure 1 Schematic of experimental technique. (A) Cue screens and intervals are illustrated. **(B)** A simplified schematic of the recording setup. The subject with implanted subdural electrode squeezes force transducers as cued by the paradigm. The neural signals, force transducer signals, and cue timestamps are simultaneously recorded on a portable computer. The intertrial interval durations are randomized per trial, while the Go/No Go and Feedback durations are adjusted per subject after a training session establishes how quickly the subject could perform the task.

minimize the time during which the dura is open, to potentially reduce brain shift. In some subjects, median nerve somatosensory evoked potential phase-reversal was used to confirm that electrodes straddled the central sulcus (Kondylis *et al.*, 2016; Randazzo *et al.*, 2016). A referential montage was used with the reference electrode placed at the left mastoid and a ground electrode placed on the shoulder. Anti-parkinsonian and anti-tremor medications were typically held for at least 12 h prior to intraoperative testing. Data analyzed for this study were obtained after the DBS electrode was placed and clinical stimulation testing was completed. Subjects were fully awake and no medication was given during task performance. Four subjects with Parkinson's disease and five subjects with essential tremor underwent bilateral subthalamic nucleus or ventral intermediate nucleus DBS lead placement, respectively, and ECoG recordings were obtained during task performance from both hemispheres in all subjects except one, in whom unilateral recordings from the first side were obtained. In subjects with no movement disorder, ECoG data were recorded 1–5 days postoperatively using standard (2.3 mm exposed disc) subdural electrode arrays (Ad-Tech, Medical Instrument Corporation). Two inverted subdural contacts served as ground and reference electrodes in these subjects. For all subject groups, ECoG signals were filtered (0.3–250 Hz, 60/120/180 Hz notch), amplified and digitized at 1000 Hz using a Grapevine neural interface processor (Ripple Inc.).

The task paradigm was implemented using Psychophysics Toolbox (Brainard, 1997) on a portable computer. Force signals from the handgrips and time stamps marking the presentation of visual cues were digitally recorded simultaneously with the ECoG signals. Grip force onsets were calculated off-line by smoothing force signals (15 ms running average) and

using a 50 N/s threshold to detect changes in the rate of force generation. The onset of derived grip force data were used to segment ECoG data, and the time stamps were used to isolate successful, contralateral Go trials.

Electrode localization

Electrodes implanted in subjects without a movement disorder were localized through co-registration of post-implantation CT images and a preoperative MRI volume. Electrode locations were then projected onto a reconstructed 3D cortical surface for visualization using a method adapted from Hermes *et al.* (2010). Subdural electrode strips temporarily implanted in the subjects with movement disorders were localized using a novel method aligning preoperative MRI, intraoperative fluoroscopy and postoperative CT (Randazzo *et al.*, 2016). Briefly, the CT and MRI were co-registered using mutual information in the SPM software package and rendered into 3D skull and brain surfaces using Osirix and Freesurfer software (Dale *et al.*, 1999), respectively. These surfaces and the fluoroscopy image were then loaded into a custom Matlab user interface and aligned using common landmarks: stereotactic frame pins, implanted depth electrodes, and skull outline (Supplementary Fig. 1). The parallax effect of the fluoroscopic images was accounted for by using the measured distance from the radiation source to the subject's skull to adjust the projection of the skull/brain surfaces. Based on the surfaces/fluoroscopic image alignment, a 3D location for each electrode was projected from the fluoroscopic image onto the cortical surface. For group analysis, electrodes were transformed onto the ICBM152 population-averaged cortical surface using surface-based normalization (Saad and Reynolds, 2012).

Electrode selection

Subdural electrodes were localized for all six subjects without a movement disorder, for 6/9 subjects with essential tremor, and for 8/11 subjects with Parkinson's disease. In the remaining subjects, for whom the anatomic location of electrodes could not be precisely localized because post-operative MRI was contraindicated or not obtained (the subject had a cardiac pacemaker, etc.) ($n = 5$) or the intraoperative fluoroscopic images were not saved by the radiology technician ($n = 1$). Two functional regions of interest were defined: areas that exhibited handgrip-specific high frequency activation, and the surrounding penumbra in which only low-frequency desynchronization specific to hand motor activity was observed. Each electrode location was transformed to the ICBM152 standardized anatomy. Based on segmentation of this standardized anatomy (Fonov *et al.*, 2009, 2011), each electrode was assigned to a Brodmann area. Electrode contacts localized to Brodmann areas 1 through 6 and to one of the functional regions of interest were included for analysis. None of these electrodes required omission from analysis due to spikes, epileptiform activity, or inadequate signal to noise ratio in the data.

Signal processing

To minimize noise and ensure recordings were comparable across acquisition environments, local field potential signals were re-referenced offline to a bipolar montage by referencing each contact to its immediate posterior neighbour, thus sacrificing one electrode per row (de Hemptinne *et al.*, 2015). For spectral analysis, local field potential and force signals were segmented into 500 ms epochs shifted by 250 ms from −1250 ms to 1250 ms relative to grip onset. This resulted in a total of nine trial epochs with 50% overlap, including four pre-movement epochs, four post-movement epochs and one mixed perimovement epoch. A pre-movement baseline epoch for each trial was segmented by capturing the 500 ms preceding the instruction cue.

The power spectral density (PSD) was calculated for all baseline and trial epochs with the Welch periodogram method (Matlab function pwelch) using a fast Fourier transform of 256 points and 50% overlap with a Hanning window to reduce edge effects. The activation weight was calculated for the alpha (8–12 Hz), low beta (13–20 Hz), high beta (21–35 Hz) and high frequency (76–115 Hz) bands by statistically comparing the PSD in each band and epoch to the PSD for the corresponding band in the baseline epoch, as has been previously described (Miller *et al.*, 2007). This measure is a signed squared cross-correlation value calculated for each trial from the PSD of the given frequency band and measures how the variance in power across the trial and baseline epochs is accounted for by the difference in mean power between them. The sign is retained, so synchronization may be distinguished from desynchronization. The frequency of maximum desynchronization was calculated for each trial as the frequency in the alpha and beta bands at which difference between the power spectral density of the test and baseline epochs was greatest.

The phase-amplitude coupling was calculated for each electrode and each trial epoch by adapting a previously described method (Tort *et al.*, 2008). First, segmented local field potential signals were bandpass filtered into three low frequency bands (alpha, low beta, high beta, as above) and 12 frequency bands in the broadband gamma range (50 to 200 Hz, logarithmically increasing step size) using a finite impulse response filter (function eegfilt from the Matlab toolbox eeglab). Next, the instantaneous phase was extracted from the low frequency bandpass filtered signals, and the instantaneous amplitude was extracted from the high frequency bandpass filtered signals using the Hilbert transform (Matlab function hilbert). The phase and amplitude were concatenated across trials to create a single continuous phase signal and a single continuous amplitude signal for each epoch and each electrode. The phase was divided into 20° bins and the distribution of the amplitude envelope across these bins was calculated. The preferred phase of coupling was defined as the phase bin with the highest amplitude. The phase-amplitude coupling was determined by calculating the entropy of this distribution and normalizing to the maximum entropy value, yielding the Modulation Index (MI) of coupling (Tort *et al.*, 2008). The MI was z-scored using the mean and standard deviation of 1000 surrogates created by recombining the instantaneous phase and amplitude with random time lags. Multiple comparisons were accounted for using false discovery rate, and for the purposes of group analysis, MI z-scores not achieving the resulting threshold for significance (z-score > 3.2) were reassigned a score of 0.

Motor performance outcomes

Task performance was assessed by measuring trial error rate, reaction time, time to peak force, maximum force, and rate at which maximum grip force was generated. The error rate was calculated as the per cent of total trials that were registered as error trials. The reaction time for each trial was the time difference between the Go cue and grip force onset, which was detected automatically by finding where the rate of change in the smoothed (100 ms smoothing window) transduced force signal exceeded 300 N/s and verified by manual inspection. The time to peak force was measured as the time from movement onset until maximum grip force. For subsequent analysis, to test motor effort and minimize the contribution of differences in baseline strength among subjects, the force profile for each trial was normalized to the average maximum force for each hand on a per subject basis. The grip force rate was calculated for each trial from both the raw and normalized force profiles by calculating the discrete time derivative of each force profile using a 10-ms step size. The maximum of this derivative was reported as the maximum grip force rate, a measure of how quickly the subject accelerated towards his or her maximum grip force. This measure was used instead of movement time to avoid the potential confounding effects of different levels of overall effort between subjects.

Statistical analysis

Lilliefors' composite goodness-of-fit test was used to test for normality in each data set. The force and reaction time data for the experimental groups were not normally distributed, so the Kruskal-Wallis one-way ANOVA was used to analyze motor performance. Movement related desynchronization and decoupling were calculated per trial as the activation weight of each epoch and the difference phase-amplitude

coupling between each epoch and the baseline epoch. These data were summarized for each electrode by the average across trials and grouped by diagnosis, functional electrode group, and frequency band. The functional groups included electrodes that recorded movement-related high frequency synchronization and electrodes that recorded only movement-related desynchronization. These data were not normally distributed, so Kruskal-Wallis one way analysis of variance was used to assess significant differences in the frequency and amplitude of maximum desynchronization, and rank-sum tests were used to assess for significant movement-related desynchronization and decoupling in each epoch, and significant differences in movement-related desynchronization and decoupling between experimental groups. A threshold α of 0.05 was set for all tests, and multiple comparisons were accounted for using Bonferroni correction, resulting in an adjusted α of 0.0019 and 0.015 for within-group and between-group analyses, respectively. The preferred phase of coupling was treated as a circular distribution and analyzed using the CircStat toolbox in Matlab (Berens, 2009). The Hodges-Ajne test was selected to assess the uniformity of phase preference distributions because it does not assume a unimodal distribution (Zar, 1999).

Results

Motor Performance

Twenty-six subjects were studied, including 11 with Parkinson's disease (three female, aged $64 \pm$ nine years), nine with essential tremor (two female, aged 68 ± 6 years), and six subjects without a movement disorder (four female, aged 33 ± 12 years). Characteristics of the study subjects are provided in Table 1. To minimize differences in task performance due to deficits of internal cueing mechanisms in subjects with Parkinson's disease (Majsak *et al.*, 1998), we administered an externally cued task that required a simple unilateral handgrip movement. An instructed delay allowed for the temporal sequencing of movement planning and execution. To determine if movement responses were similar between subjects in the three groups, we analyzed the trial error rate, reaction time, time to peak force, maximum force, and rate at which maximum grip force was generated. There was no significant difference (Kruskal Wallis, $P > 0.4$) in any of these measures, between subjects with Parkinson's disease and essential tremor, or between subjects with a movement disorder and those without. These data are shown at group level in Supplementary Table 1, and on a per subject basis in Supplementary Table 2. In addition, there was no significant difference between groups for the normalized grip force rate in the first 500 ms and no significant difference in the normalized grip force during the entire 1000 ms of the movement epoch (Supplementary Fig. 2). In summary, the motor performance of subjects with Parkinson's disease and essential tremor during this task was not statistically different from that of subjects with no movement disorder, in all domains tested.

Changes in alpha and beta oscillations relative to movement onset

In total, 21 of 26 subjects had sufficient pre- and post-operative imaging for electrode localization. Movement related desynchronization and high frequency activity from all localized electrodes were mapped onto the ICBM 152 MRI template brain volume. To determine differences in cortical activity related specifically to the coding of hand motor function, electrode locations that exhibited movement-related desynchronization were separated into the high-frequency activity zone and the low-frequency desynchronization penumbra, as high frequency activity has been shown previously to track behaviour-specific brain activation with high spatial and temporal specificity (Crone *et al.*, 1998a, 2006). High frequency activity was localized to the peri-rolandic gyri in the region of the hand knob (termed the 'high-frequency activity zone' here), with movement-related desynchronization of low frequencies appearing across a larger region including the peri-rolandic and premotor gyri surrounding the hand knob (Fig. 2, termed the 'low-frequency desynchronization penumbra' here).

Movement-related desynchronization for all subject groups spanned a broad band including 8–35 Hz (Fig. 3A). We next investigated specific associations between movement disorders and the frequency and amplitude characteristics of cortical movement related desynchronization in the alpha and beta frequency bands, in both groups of electrode locations. When considering the factors of patient diagnosis and electrode localization within high frequency zone versus low frequency penumbra, there were significant differences in the frequency and amplitude of maximum desynchronization (Kruskal Wallis $P < 1 \times 10^{-3}$, $P < 1 \times 10^{-12}$). As demonstrated in Fig. 3B, the frequency of maximum desynchronization was significantly (Bonferroni corrected $P < 0.05$) greater for subjects with Parkinson's disease (median frequency in high frequency activity zone = 19.1 Hz; median frequency in low frequency desynchronization penumbra = 17.1 Hz) compared to both subjects with essential tremor (median frequency in high frequency activity zone = 17.4 Hz; median frequency in low frequency desynchronization penumbra = 13.6 Hz) and subjects with no movement disorder (median frequency in high frequency activity zone = 16.1 Hz; median frequency in low frequency desynchronization penumbra = 12.3 Hz). The frequency of maximum desynchronization was significantly greater for electrodes in the high frequency activity zone compared to the low frequency desynchronization penumbra, only in the group with no movement disorder. As demonstrated in Fig. 3C, the amplitude of maximum desynchronization was greater in subjects with movement disorders than in controls without a movement disorder, and was greater in the high frequency activity zone than in the low frequency penumbra for subjects with a movement disorder.
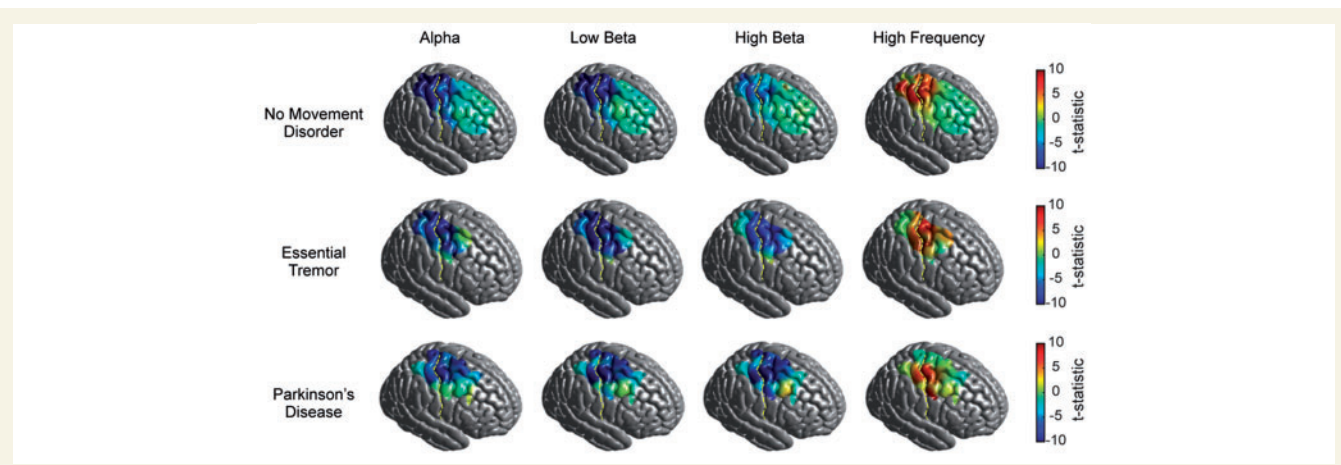
Figure 2 Movement-locked activation mapped onto standardized anatomy for each frequency band and experimental group.
A *t*-test of activation weights at movement onset across successful, contralateral Go trials was conducted for all electrodes that were localized and analyzed. The data plotted at each cortical location reflects the weighted average of t-statistics from electrodes located within a 2-cm radius, after transforming electrode locations onto the ICBM152 cortical surface. At each vertex on the cortical surface, a weight of 1 was assigned to t-statistics from electrodes with a distance <0.5 cm from the given vertex, and exponentially decreasing weights from 1 to 0 were assigned to t-statistics from electrodes with distances from 0.5 to 2 cm.
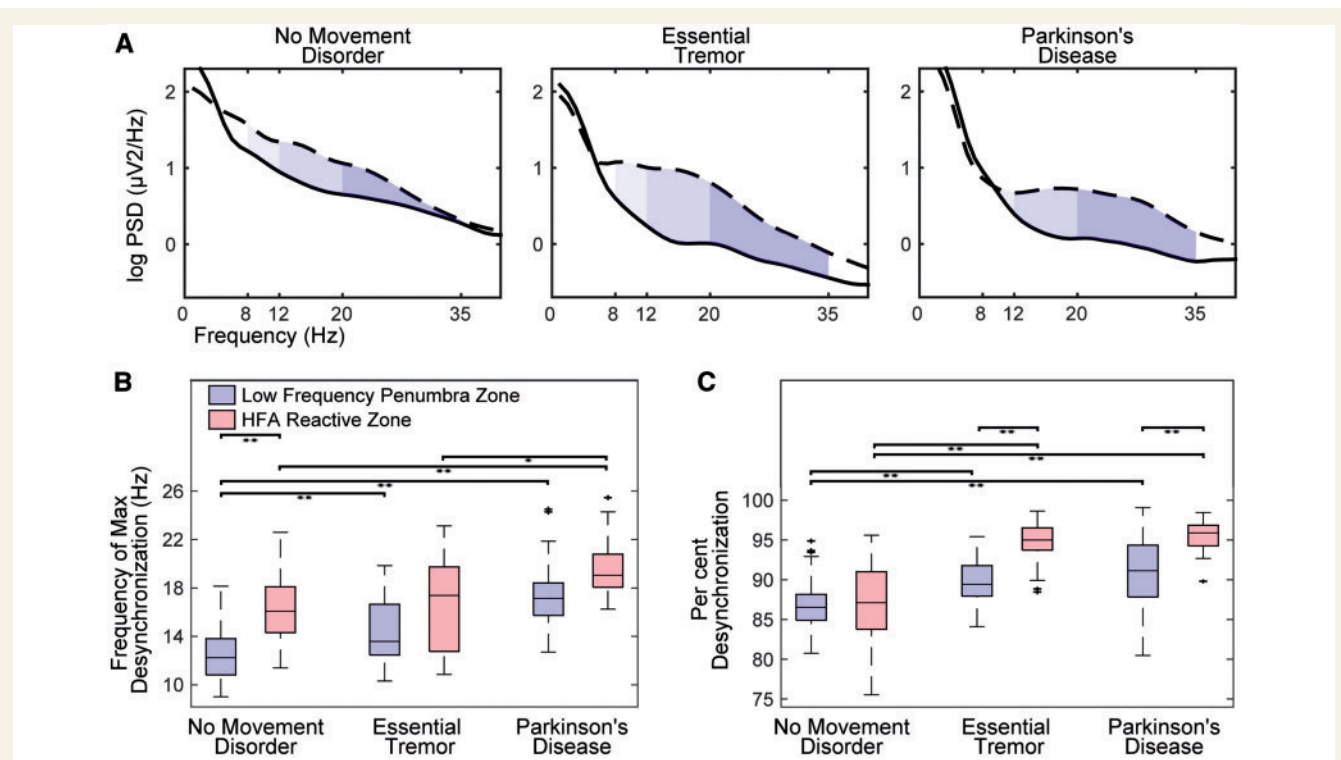

Figure 3 Movement-related changes in cortical power spectra. (**A**) Average power spectra during movement (solid line, 500 ms window following movement onset) and baseline (dotted line, 500 ms window preceding instruction cue) for electrodes in the high frequency activity (HFA) zone for each experimental group. The power decrease between the baseline and movement epochs is highlighted by the blue shading, with the light, medium, and dark blue representing the alpha, low beta and high beta frequency bands, respectively. (**B**) Box plot indicating the frequency of maximal desynchronization, calculated by determining the frequency point on the power spectrum for each trial where the difference between movement and baseline was greatest, and then averaging across trials for each electrode. (**C**) Box plot indicating the per cent of maximal desynchronization. This was calculated by finding, for each trial, the per cent of power change at the frequency of maximum desynchronization during the movement epoch, and then averaging across trials for each electrode. In **B** and **C**, differences between groups were assessed using Kruskal-Wallis one-way ANOVA with six groups including the combinations of experimental group and activation zones. Bonferroni correction for multiple comparisons was applied, and significant differences are reported at $^{*}P < 0.05$ and $^{**}P < 0.01$.
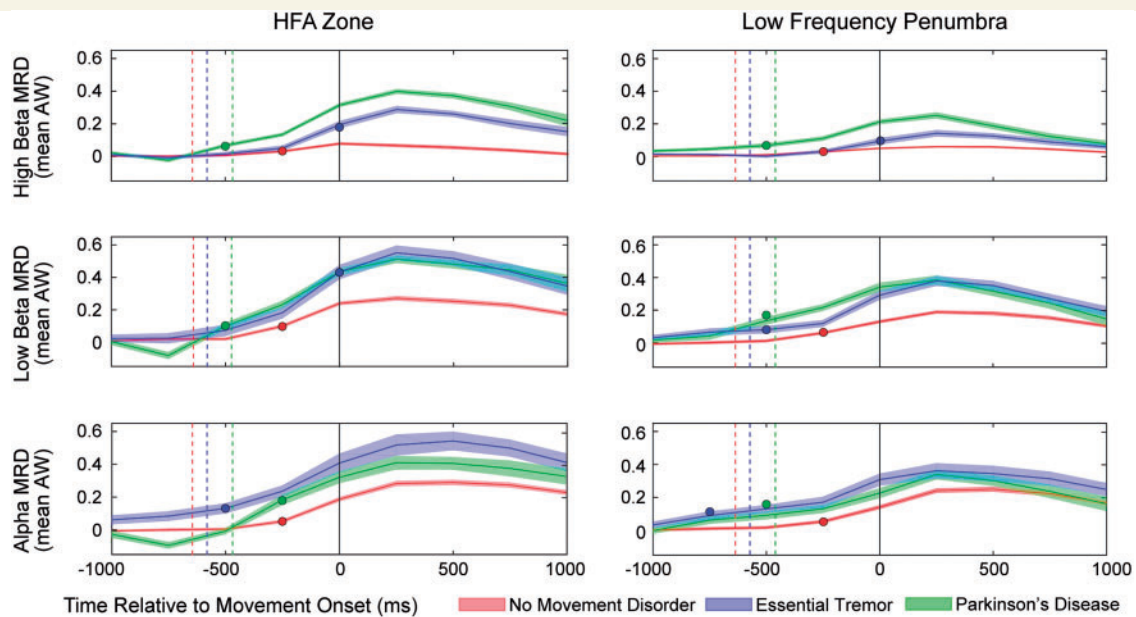
Figure 4 Evolution of low frequency band power during preparation and execution of movement. The mean ± standard error of the mean (SEM) of alpha (*bottom*), low beta (*middle*) and high beta (*top*) desynchronization in the high frequency activity (*left*) and low frequency penumbra (*right*) zones, is shown centred on movement onset for each experimental group (epilepsy, red; Parkinson's disease, green; essential tremor, blue). Circles represent the time point at which desynchronization became significant for each experimental group. Dashed lines indicate the estimated Go cue presentation, based on average reaction time for each experimental group.

We next investigated associations between movement disorders and the magnitude and timing of movement-related desynchronization relative to the onset of movement for cortical locations (Fig. 4). Movement-related desynchronization achieved a greater magnitude at movement onset in subjects with movement disorders compared to those without movement disorders (rank-sum Bonferroni corrected $P < 0.05$), and was of even greater magnitude in the high frequency activity zone compared to the low-frequency penumbra within each group (rank-sum Bonferroni corrected $P < 0.05$). There was no statistical difference between the timing of the onset of movement-related desynchronization in any group.

Changes in alpha and beta phase coupling to gamma amplitude relative to movement

In all subject groups, there was significant (Bonferroni corrected $P < 0.05$) coupling of the phase of both alpha and beta bands to the amplitude of gamma activity at rest, in the high frequency activation zone. Subjects with Parkinson's disease and essential tremor, however, exhibited significantly more phase-amplitude coupling at rest than subjects without movement disorders (Fig. 5). In Parkinson's disease, the magnitude of phase-amplitude coupling at rest was greatest for high-beta, which was coupled with broadband gamma (60–200 Hz), while the coupling of low-beta was greatest to frequencies in a narrower range
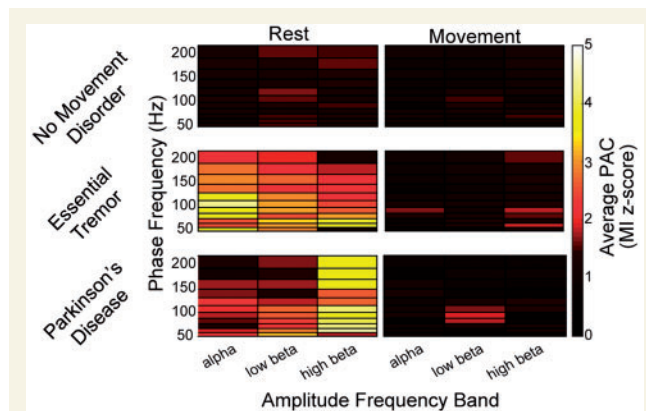

Figure 5 Phase–amplitude coupling at rest and during movement. The z-score of modulation index (Tort *et al.*, 2008) after correction for multiple comparisons using 1000 surrogates was calculated for each electrode and each phase/amplitude frequency pair. These z-scores were averaged for all electrodes in the high frequency activity zone for each experimental group, during the 500 ms baseline epoch and during the first 500 ms of movement execution.

between 60–120 Hz. In essential tremor, the magnitude of phase-amplitude coupling at rest to broadband gamma was significantly (Bonferroni corrected $P < 0.05$) greater than during movement for both low- and high-beta, but the strongest effect was seen for alpha. Coupling of low-beta was not restricted to the lower gamma range, as observed in subjects with Parkinson's disease. In subjects without

movement disorders, phase-amplitude coupling to broadband gamma at rest reached significance for low- and high-beta, but with much smaller magnitudes. While phase-amplitude coupling at rest was significantly greater in subjects with movement disorders (*post hoc* rank-sum, $P < 0.05$), there was no significant difference among experimental groups in the proportion of electrodes in the high frequency activation zone that recorded significant phase-amplitude coupling (Kruskal-Wallis, $P > 0.05$). In one subject ECoG was recorded from a high density grid with smaller contact surface areas and inter-electrode distances. The total magnitude of phase-amplitude coupling and the proportion of electrodes recording significant phase-amplitude coupling from the high density strip fell within the respective ranges for recordings from standard electrode strips (Supplementary Fig. 3). We frequently observed regional differences in the preferred phase of coupling as well as a partial reversal across the central sulcus (Supplementary Fig. 4). The distribution of phase preference was non-uniform only in the essential tremor group (Hodjes-Ajne, $P < 0.05$) (Supplementary Fig. 5).

We found that phase-amplitude coupling was attenuated during movement. Phase-amplitude decoupling in the high

frequency activity zone occurred simultaneously with the emergence of movement-related desynchronization and high frequency activity (see example in Fig. 6). Next we explored the temporal dynamics of phase-amplitude decoupling in relation to movement onset for each frequency band and subject group (Fig. 7). In subjects without a movement disorder, phase-amplitude decoupling was not strong enough to reach significance (rank-sum Bonferroni corrected $P < 0.05$) prior to movement onset and then only achieved the threshold for significance briefly in the low-beta frequency band, immediately following movement onset. In contrast, phase-amplitude decoupling occurred earlier and more robustly in subjects with Parkinson's disease and essential tremor, becoming significant at least 250 ms before movement onset and persisting through the duration of movement. Notably, only Parkinson's subjects exhibited significant decoupling of high-beta phase from gamma amplitude before the onset of movement, and only essential tremor subjects exhibited significant decoupling of alpha, while both exhibited significant decoupling of low-beta phase before movement. Comparison of phase-amplitude coupling between experimental groups demonstrated that decoupling in subjects
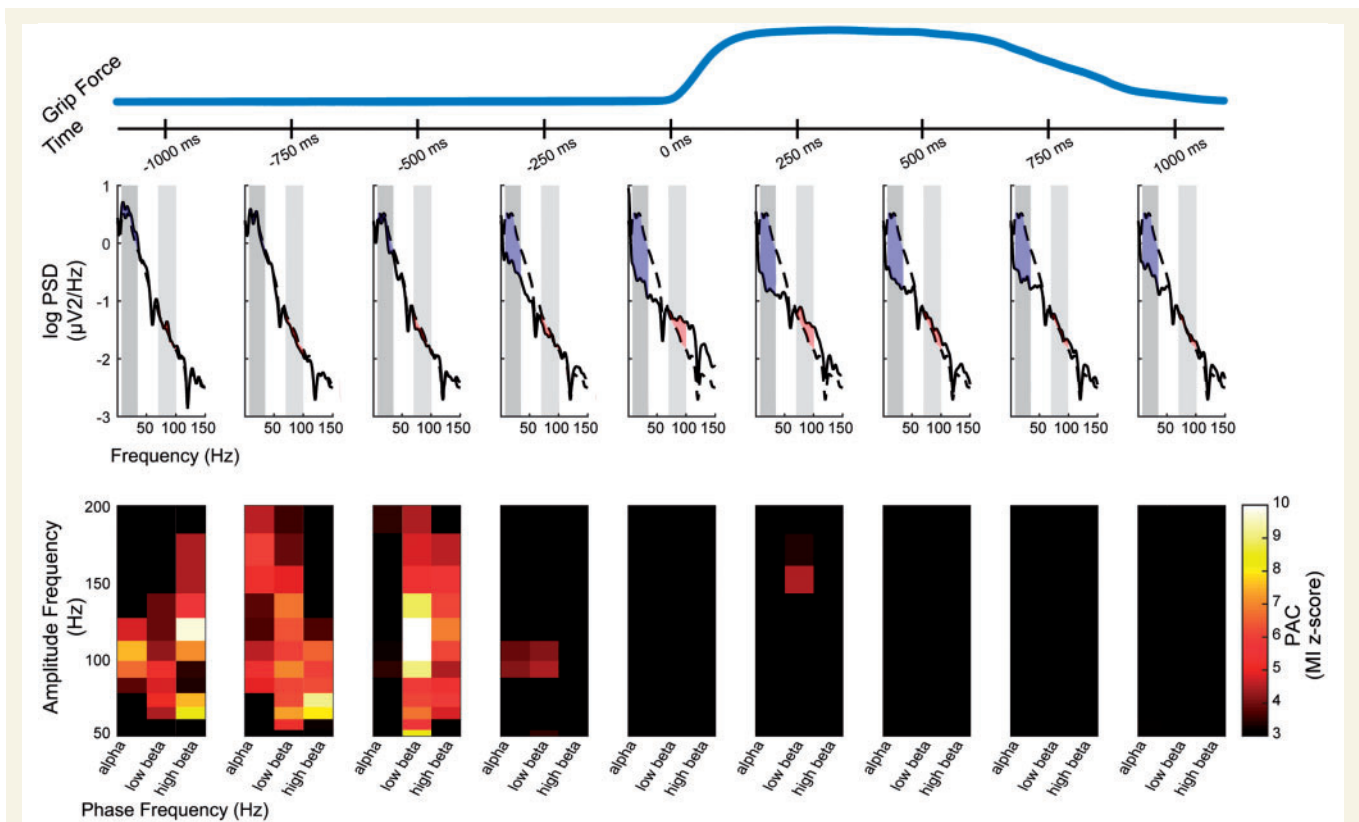

Figure 6 Evolution of spectral power and phase-amplitude coupling for a sample electrode from the high frequency activation zone in a subject with Parkinson's disease. *Top to bottom*: Grip force centred on grip onset (0 ms) and averaged across trials, power spectral density and phase–amplitude coupling for 500 ms epochs overlapping by 250 ms. The power spectral density is reported for each epoch (solid line) and changes from the baseline epoch (dotted line) are highlighted in the low frequency band (8–35 Hz, blue) and high frequency band (76–100 Hz, red).
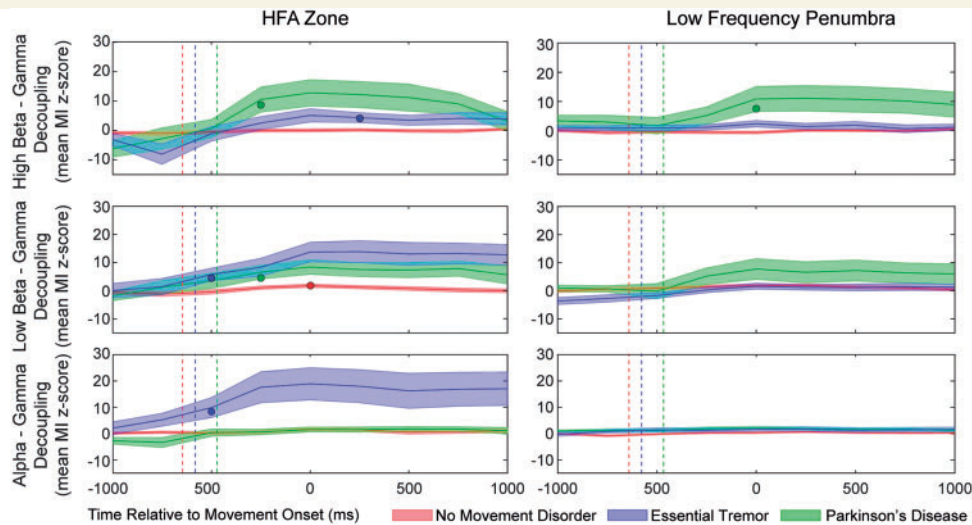
Figure 7 Evolution of phase-amplitude decoupling during movement preparation and execution. The mean ± SEM decoupling between the phase of alpha (*bottom*), low beta (*middle*) and high beta (*top*) and the amplitude of broadband high gamma activity (50–200 Hz) in the high frequency activity (*left*) and low frequency penumbra (*right*) zones for subjects in each experimental group (epilepsy, red; Parkinson's disease, green; essential tremor, blue) is shown centred on movement onset. Circles mark the time point where phase-amplitude decoupling became significant for each experimental group. Dashed lines indicate the estimated time of Go cue presentation, based on average reaction time for each experimental group.

with Parkinson's and essential tremor was significantly (Bonferroni corrected $P < 0.05$) greater in both beta phase frequencies compared to controls. Additionally, decoupling was greater in high beta phase frequency for Parkinson's compared to essential tremor, and greater in the alpha phase frequency for essential tremor compared to both other groups. the low-frequency penumbra, significant decoupling occurred only for the beta phases in the Parkinson's group and to a lesser extent than in the high frequency activation zone.

Discussion

In this study we used ECoG during DBS lead implantation surgery to record local field potentials from the sensorimotor cortex in subjects with Parkinson's disease and essential tremor during a visually cued, instructed delay, monetary incentive handgrip task. We demonstrated that a number of movement kinematic measures in subjects with these movement disorders were not significantly different from subjects without a movement disorder who performed the same task while undergoing inpatient intracranial monitoring. Initial major findings in this study are: (i) we show for the first time that abnormal cortical phase–amplitude coupling is not specific to Parkinson's disease, but also occurs in essential tremor, although most prominently for alpha rather than beta phase; (ii) robust alpha and beta desynchronization is a shared physiological mechanism for modulating abnormal neural activity in Parkinson's disease and essential tremor, with the greatest high-beta desynchronization occurring in Parkinson's disease and the greatest alpha desynchronization occurring

in essential tremor; and (iii) cortical phase–amplitude decoupling during movement is much more robust in subjects with Parkinson's disease and essential tremor than in subjects with no movement disorder, with decoupling of high-beta phase to gamma amplitude specific to Parkinson's disease and decoupling of alpha-phase to gamma amplitude specific to essential tremor. Given relatively similar motor performance between subject groups, the observation of disease-specific modulation of cortical synchrony and phase-amplitude coupling during movement suggests that the observed neurodynamics may represent functional pathways through which motor function may be normalized in movement disorders.

Alpha-gamma phase-amplitude coupling is excessive in essential tremor and Parkinson's disease

In addition to excessive coupling of the phase of beta activity to the amplitude of gamma activity at rest in Parkinson's disease subjects, as has been previously reported (de Hemptinne *et al.*, 2013), we observed excess coupling of the phase of alpha activity to the amplitude of gamma activity, indicating that abnormal coupling to gamma amplitude is not restricted to beta range frequencies in this disease. Furthermore, we found that subjects with essential tremor exhibited abnormal phase-amplitude coupling to gamma activity that occurred predominantly for alpha phase, but was also present for beta phase, indicating that excessive phase-amplitude coupling in primary motor cortex is not an observation exclusive to Parkinson's disease. Given these findings, it is possible that the alpha band effects

in both disease states reflect entrainment of the circuit at tremor frequencies (Timmermann *et al.*, 2003), given that we did not exclude Parkinson's disease patients with tremor from our analysis. In that case, the data could be interpreted to suggest that tremor-related frequencies are represented in excessive phase-amplitude coupling present at rest in both subjects with a resting tremor (Parkinson's disease) and those with an action tremor (essential tremor). One possible explanation for this apparent incongruity is that a shared manifestation of tremor at the cortical level is suggested by evidence that the basal ganglia does not drive resting tremor directly (Zaidel *et al.*, 2009), but that resting tremor results from cortex-level interactions between abnormal basal ganglia output and dysfunctional activity in the cerebello-thalamo-cortical circuit (Helmich *et al.*, 2012). With regard to the presence of excessive beta–gamma coupling in essential tremor, it is possible that this interaction represents a compensatory state for attempting to suppress tremor.

Subjects with Parkinson's disease and essential tremor can move well under certain conditions

To compare sensorimotor cortical oscillations during movement across disease states, it was important to record brain activity during a motor task for which the movement kinematics were not different between groups. Paradoxical kinesis is a term that describes the preserved ability of subjects with Parkinson's disease to move normally in particular circumstances, despite typically moving more slowly. The motor motivation hypothesis of basal ganglia function predicts that bradykinesia results from dopamine depletion-related deficits in computing the context-specific cost and reward functions needed to move at normal speed (Mazzoni *et al.*, 2007; Turner and Desmurget, 2010). Reversing pathological shifts in the cost/benefit ratio of moving fast might allow more normal movement. In support of this hypothesis, we found no significant difference in any measures of movement kinematics between subjects with Parkinson's disease in the OFF medication condition, and those with presumed normal dopamine function, during performance of a task in which correct performance was monetarily incentivized. As we also showed that subjects with essential tremor also could execute the motor task as well as subjects without a movement disorder, the similar motor performance between subject groups allowed us to observe potentially compensatory neural mechanisms that may support an ability for relatively normalized motor function in these diseases.

Movement-related cortical decoupling is amplified in both Parkinson's disease and essential tremor

We found that in order for Parkinson's and essential tremor subjects to produce movements that are kinematically similar to those of subjects without a movement disorder, movement-related desynchronization achieved greater magnitude than was required in subjects without a movement disorder. Thus, subjects with movement disorders can exaggerate a normal pattern of sensorimotor cortical neural activation typically required for movement, to improve motor function. Comparing the two movement disorders, the peak frequency of movement-related desynchronization was significantly greater in subjects with Parkinson's disease than with essential tremor. These findings are consistent with previous studies documenting baseline synchronization and movement-related desynchronization at a higher beta-range frequency in subjects with Parkinson's disease compared to subjects with essential tremor or dystonia (Crowell *et al.*, 2012).

Although the decrease in abnormal synchrony during movement in Parkinson's disease matches the finding that resting tremor is typically decreased during voluntary movements (Deuschl *et al.*, 2000), the relationship of the reduction in abnormal synchrony in essential tremor to motor pathology, the action tremor, is less clear. Our task was not designed to measure the extent of tremor during ongoing movement. With regard to Parkinson's disease, it has been suggested that striato-pallidal activity necessary for tremor can only emerge under motorically static conditions when the basal ganglia are not involved in voluntary motor behaviour (Helmich *et al.*, 2012). The reduction of abnormal synchrony in the essential tremor group during intentional movement, which might be expected to elicit action tremor, suggests that no tremor was produced with the simple movement used in this study, that the motor circuits engaged to produce the measured movement characteristics are different than that of the action tremor oscillator itself, or that tremor produces beta desynchronization similar to that which occurs with normal movement. With respect to the later possibility, Qasim *et al.* (2016), however, have provided evidence that spontaneous resting tremor is associated with reduced cortical beta power, cortical–cortical coherence and phase–amplitude coupling in subjects with Parkinson's disease. Although we did not perform simultaneous electromyography in the current subjects, doing so is a high priority for future studies to directly assess the interaction between the action tremor, voluntary motion, and cortical synchrony.

We found that the amount of movement related phase-amplitude decoupling was much greater in movement disorders subjects, which reflected the increased phase-amplitude coupling at rest and mirrored the disease specificity found for movement-related desynchronization. The phase–amplitude decoupling for the alpha phase frequency range was significant only in subjects with essential tremor. The apparent differences in narrow bands of significant alpha phase-amplitude coupling observed in with Parkinson's disease group (Fig. 6) did not withstand statistical testing. Parkinson's disease subjects further exhibited significant decoupling of high-beta phase from gamma amplitude, again reflecting the idea that the frequency range of oscillations within the beta band in the basal

ganglia–thalamocortical circuit may be increased in the parkinsonian state (Crowell *et al.*, 2012). The functional distinction between low and high-beta rhythms is not clear, although the low-beta rhythm has a greater baseline sensitivity to levodopa than the high-beta (Priori *et al.*, 2004; Foffani *et al.*, 2005). Our data suggest that high and low beta oscillations may represent functionally distinct mechanisms that arise from separate oscillating networks, which summate at the recording site. Thus the gamma amplitude signal consists of multiple oscillating components, each coupled to the phase of a distinct beta oscillator network.

There were no significant peaks in preferred phase of coupling in the Parkinson's disease and non-movement disorder groups, likely due to the frequently observed regional variance and partial reversal of phase preference frequently observed across the central sulcus. Additional variance is added by the broad band of amplitude frequencies tested, which likely encompasses multiple oscillating components coupling to distinct phase frequencies and with different phase preferences. The significant peak in essential tremor may reflect decreased regional variation in the preferred phase of coupling and warrants further investigation.

Both movement disorders groups demonstrated significant decoupling of low-beta phase from gamma amplitude, reflecting a relatively more normal movement-related physiology, as evidenced by the finding that the only significant decoupling observed in subjects with no movement disorder was that of low-beta phase decoupling observed in the high frequency activation zone. These data also demonstrate that phase-amplitude decoupling is a more specific mechanistic biomarker for movement than general band power desynchronization, given that movement-related desynchronization was evident across both the high frequency activity zone and low-frequency penumbra, while decoupling was important only within the high frequency activity zone itself. This finding is consistent with previous work demonstrating that movement related decoupling is not reliably correlated with decreased band power of the lower frequency at cortical sites activated during movement (Miller *et al.*, 2012), and supports the finding that the therapeutic effect of DBS in Parkinson's disease is related specifically to decreased beta phase amplitude decoupling and not to beta desynchronization (de Hemptinne *et al.*, 2015).

Study limitations

We recorded local field potential activity from the cortex of movement disorders subjects acutely in the operating room, and epilepsy subjects subacutely in the epilepsy monitoring unit. The effects of different recording environments are potential confounders of the analysis of these signals. This limitation was addressed by applying bipolar montages to better isolate local signals, and by constraining analysis to changes from baseline rather than to absolute measures of spectral power. We also acknowledge that although interictal recordings in epilepsy subjects are the closest we have to normal control data for invasive recordings

in humans with movement disorders, these data may not represent the normal state of the motor system, even in regions outside of the seizure onset zone, due to the effects of chronic anti-epileptic medication use. In deep brain stimulation patients, in order to ensure that clinically essential work was completed prior to the research component, and to make recordings after the longest possible interval after stopping sedation, recordings were made after lead insertion. Lead insertion, however, may have significant effects on physiology, given that a significant reduction in the action tremor in patients with essential tremor after lead insertion alone is not uncommon in clinical practice. In all DBS subjects, anatomical localization of temporarily implanted subdural contacts was limited by the absence of intraoperative CT imaging, which is not available at our institution. We addressed this by developing a novel technique using lateral fluoroscopic imaging that allows us to localize subdural contacts to within a few millimeters (Kondylis *et al.*, 2016; Randazzo *et al.*, 2016).

Conclusions

These results demonstrate that subjects with Parkinson's disease and essential tremor can produce vigorous movement by reversing excess sensorimotor cortical synchrony and phase–amplitude coupling that are hallmarks of these disease states. These data are suggestive of a compensatory mechanisms through which subjects with these two movement disorders may normalize motor behaviour.

Acknowledgements

Funding

Supplementary material

Supplementary material is available at *Brain* online.

References

Air EL, Ryapolova-Webb E, de Hemptinne C, Ostrem JL, Galifianakis NB, Larson PS, et al. Acute effects of thalamic deep brain

stimulation and thalamotomy on sensorimotor cortex local field potentials in essential tremor. Clin Neurophysiol 2012; 123: 2232–8.

Berens P. CircStat: a MATLAB toolbox for circular statistics. J Stat Softw 2009; 31: 1–21.

Bosboom JLW, Stoffers D, Stam CJ, van Dijk BW, Verbunt J, Berendse HW, et al. Resting state oscillatory brain dynamics in Parkinson's disease: an MEG study. Clin Neurophysiol 2006; 117: 2521–31.

Brainard D. The psychophysics toolbox. Spat Vis 1997; 10: 433–6.

Crone NE, Miglioretti DL, Gordon B, Lesser RP. Functional mapping of human sensorimotor cortex with electrocorticographic spectral analysis: II. Event-related synchronization in the gamma band. Brain 1998a; 121: 2301–15.

Crone NE, Miglioretti DL, Gordon B, Sieracki JM, Wilson MT, Uematsu S, et al. Functional mapping of human sensorimotor cortex with electrocorticographic spectral analysis: I. Alpha and beta event-related desynchronization. Brain 1998b; 121 (Pt 12): 2271–99.

Crone NE, Sinai A, Korzeniewska A. High-frequency gamma oscillations and human brain mapping with electrocorticography. Prog Brain Res 2006; 159: 275–95.

Crowell AL, Ryapolova-Webb ES, Ostrem JL, Galifianakis NB, Shimamoto S, Lim DA, et al. Oscillations in sensorimotor cortex in movement disorders: an electrocorticography study. Brain 2012; 135: 615–30.

Dale AM, Fischl B, Sereno MI. Cortical surface-based analysis: I. Segmentation and surface reconstruction. Neuroimage 1999; 9: 179–94.

Deuschl G, Raethjen J, Baron R, Lindemann M, Wilms H, Krack P. The pathophysiology of parkinsonian tremor: a review. J Neurol 2000; 247: V33–48.

Foffani G, Bianchi AM, Baselli G, Priori A. Movement-related frequency modulation of beta oscillatory activity in the human subthalamic nucleus. J Physiol 2005; 568: 699–711.

Fonov V, Evans A, McKinstry R, Almli C, Collins D. Unbiased nonlinear average age-appropriate brain templates from birth to adulthood. Neuroimage 2009; 47: S102.

Fonov V, Evans AC, Botteron K, Almli CR, McKinstry RC, Collins DL. Unbiased average age-appropriate atlases for pediatric studies. Neuroimage 2011; 54: 313–27.

Hellwig B, Häußler S, Schelter B, Lauk M, Guschlbauer B, Timmer J, et al. Early report tremor-correlated cortical activity in essential tremor. Lancet 2001; 357: 519–23.

Helmich RC, Hallett M, Deuschl G, Toni I, Bloem BR. Cerebral causes and consequences of parkinsonian resting tremor: a tale of two circuits? Brain 2012; 135: 3206–26.

de Hemptinne C, Ryapolova-Webb ES, Air EL, Garcia PA, Miller KJ, Ojemann JG, et al. Exaggerated phase-amplitude coupling in the primary motor cortex in Parkinson disease. Proc Natl Acad Sci USA 2013; 110: 4780–5.

de Hemptinne C, Swann NC, Ostrem JL, Ryapolova-Webb ES, San Luciano M, Galifianakis NB, et al. Therapeutic deep brain stimulation reduces cortical phase-amplitude coupling in Parkinson's disease. Nat Neurosci 2015; 18: 779–86.

Hermes D, Miller KJ, Noordmans HJ, Vansteensel MJ, Ramsey NF. Automated electrocorticographic electrode localization on individually rendered brain surfaces. J Neurosci Methods 2010; 185: 293–8.

Jasper H, Penfield W. Electrocorticograms in man: effect of voluntary movement upon the electrical activity of the precentral gyrus. Arch Psychiatr Nervenkr 1949; 183: 163–74.

Kondylis ED, Randazzo MJ, Alhourani A, Wozny TA, Lipski WJ, Crammond DJ, et al. High frequency activation data used to validate localization of cortical electrodes during surgery for deep brain stimulation. Data Brief 2016; 6: 204–7.

Majsak M, Kaminski T, Gentile A, Flanagan J. The reaching movements of patients with Parkinson's disease under self-determined maximal speed and visually cued conditions. Brain 1998; 121 (Pt 4): 755–66

Mazzoni P, Hristova A, Krakauer JW. Why don't we move faster? Parkinson's disease, movement vigor, and implicit motivation. J Neurosci 2007; 27: 7105–16.

Miller KJ, Hermes D, Honey CJ, Hebb AO, Ramsey NF, Knight RT, et al. Human motor cortical activity is selectively phase-entrained on underlying rhythms. PLoS Comput Biol 2012; 8: e1002655

Miller KJ, Leuthardt EC, Schalk G, Rao RPN, Anderson NR, Moran DW, et al. Spectral changes in cortical surface potentials during motor movement. J Neurosci 2007; 27: 2424–32.

Priori A, Foffani G, Pesenti A, Tamma F, Bianchi AM, Pellegrini M, et al. Rhythm-specific pharmacological modulation of subthalamic activity in Parkinson's disease. Exp Neurol 2004; 189: 369–79.

Qasim SE, de Hemptinne C, Swann NC, Miocinovic S, Ostrem JL, Starr PA. Electrocorticography reveals beta desynchronization in the basal ganglia-cortical loop during rest tremor in Parkinson's disease. Neurobiol Dis 2016; 86: 177–86.

Raethjen J, Govindan RB, Kopper F, Muthuraman M, Deuschl G. Cortical involvement in the generation of essential tremor. J Neurophysiol 2007; 97: 3219–28.

Randazzo MJM, Kondylis EDE, Alhourani A, Wozny TA, Lipski WJ, Crammond DJ, et al. Three-dimensional localization of cortical electrodes in deep brain stimulation surgery from intraoperative fluoroscopy. Neuroimage 2016; 125: 515–21.

Saad ZS, Reynolds RC. Suma. Neuroimage 2012; 62: 768–73.

Schnitzler A, Münks C, Butz M, Timmermann L, Gross J. Synchronized brain network associated with essential tremor as revealed by magnetoencephalography. Mov Disord 2009; 24: 1629–35.

Timmermann L, Gross J, Dirks M, Volkmann J, Freund H-J, Schnitzler A. The cerebral oscillatory network of parkinsonian resting tremor. Brain 2003; 126: 199–212.

Tort ABL, Kramer MA, Thorn C, Gibson DJ, Kubota Y, Graybiel AM, et al. Dynamic cross-frequency couplings of local field potential oscillations in rat striatum and hippocampus during performance of a T-maze task. Proc Natl Acad Sci USA 2008; 105: 20517–22.

Turner RS, Desmurget M. Basal ganglia contributions to motor control: a vigorous tutor. Curr Opin Neurobiol 2010; 20: 704–16.

Yanagisawa T, Yamashita O, Hirata M, Kishima H, Saitoh Y, Goto T, et al. Regulation of motor representation by phase-amplitude coupling in the sensorimotor cortex. J Neurosci 2012; 32: 15467–75.

Zaidel A, Arkadir D, Israel Z, Bergman H. Akineto-rigid vs. tremor syndromes in Parkinsonism. Curr Opin Neurol 2009; 22: 387–93.

Zar JH. Biostatistical analysis. Upper Saddle River, NJ: Prentice Hall; 1999.